

Bulk Measurement of the Franz-Keldysh Effect in Si*

YIZHAK YACOBY

Massachusetts Institute of Technology, Cambridge, Massachusetts

(Received 25 May 1965; revised manuscript received 13 September 1965)

Results of bulk measurements of the Franz-Keldysh effect in Si at -35°C and -191°C are presented in this paper. Use is made of a special-purpose computer in order to obtain very long integration time without drift, which in turn made the performance of a high-resolution measurement possible. The measured change in absorption caused by the applied electric field as a function of photon energy displays considerably more structure than previously reported. The position of the different peaks in photon energy is found to be independent of the applied electric field. Consequently, the peaks are interpreted as different phonon processes. The absolute value of the change in absorption was found to be proportional to the applied electric field to the 1.72 power which is closer to the theoretically expected value of 1.33 than is the value of 2 previously reported.

INTRODUCTION

RECENT experimental observations of the Franz¹-Keldysh² effect in Si made by Chester and Wendland³ and especially by Frova and Handler⁴ show that this effect might be a very powerful tool in the analysis of the different processes taking part in the indirect optical absorption in Si.

Tunneling measurements made by Chynoweth *et al.*⁵ in Si show a large number of phonon-assisted tunneling processes, in addition to the ones observed by Frova and Handler in the measurement of the Keldysh effect. This raises the question whether the additional tunneling processes could be observed also in optical transitions by means of a higher resolution and more sensitive measurement of the Franz-Keldysh effect.

As a means of obtaining higher sensitivity in the measurement of the change in absorption $\Delta\alpha$ produced by applied electric field, as a function of photon energy ϵ_i , we use very long integration times in a special way which also avoids drift. In this manner we are able to resolve a significantly larger number of positive peaks than have previously been reported.

Theory⁶ predicts that for *each* absorption process $\Delta\alpha$ as a function of ϵ_i should display a series of peaks, the first one being just above the absorption edge and the others at higher energies. Thus, special care should be taken to determine whether several of the peaks observed belong to the same process. This was done by repeating the measurement at different electric field intensities.

To assist in the interpretation of the results, the

measurement was also performed at a low temperature, namely -191°C .

The dependence of the change in absorption upon the applied field as compared to theory is of particular importance for the understanding of the nature of the observed results. In the present work the electric field was applied to the bulk of the sample and in a special way so as to have high reliability in the determination of the applied field. Moreover, higher resolution was used in the measurement of $\Delta\alpha$ versus field than was used in the measurement of $\Delta\alpha$ as a function of ϵ_i , in order to obtain a better measure of the absolute value of the field effect. The results show that $\Delta\alpha \propto E^{1.72}$, a dependence which is considerably different from the E^2 dependence previously reported^{3,4} and which is also much closer to the theoretical prediction of $E^{4/3}$.^{6,7}

The following sections describe the experimental procedure, the results, and their interpretation. A few concluding remarks are given in the last section.

EXPERIMENTAL PROCEDURE

In applying the electric field to the bulk, one confronts several problems: (1) Heating is produced by ohmic losses. (2) At high electric field, injection of carriers from the metal electrodes into the semiconductor is practically unavoidable. (3) Possible surface barriers might cause a nonuniform field distribution in the sample.

To overcome these difficulties the following procedure was used in preparing the samples. High resistivity ($10^4 \Omega \text{ cm}$) *p*-type Si wafers were irradiated by fast neutrons. The irradiation increased the resistivity of the wafers via compensation⁸ to $10^5 \Omega \text{ cm}$ at 10°C . The wafers were then optically polished perpendicular to the $\langle 111 \rangle$ axis to a thickness of 100μ , and covered with a thin film of insulator (Formvar) $\sim 300\text{-\AA}$ thick. Thin Pt electrodes were then evaporated on the insulating film as shown in Fig. 1.

The electric field was applied in the form of a 200

* Research supported in part by the Advanced Research Project Agency under contract No. SD-90. This paper is based on a thesis submitted to the Massachusetts Institute of Technology in partial fulfillment of the requirements for the degree of Doctor of Science.

¹ A. Von Walter Franz, Z. Naturforsch. **13a**, 484 (1958).

² L. V. Keldysh, Zh. Eksperim. i Teor. Fiz. **34**, 1138 (1958) [English transl.: Soviet Phys.—JETP **7**, 788 (1958)].

³ M. Chester and P. H. Wendland, Phys. Rev. Letters **13**, 193 (1964).

⁴ A. Frova and P. Handler, Phys. Rev. Letters **14**, 178 (1965).

⁵ A. G. Chynoweth, R. A. Logan, and D. E. Thomas, Phys. Rev. **125**, 877 (1962).

⁶ Y. Yacoby, Phys. Rev. **140**, A263 (1965).

⁷ C. M. Penchina, Phys. Rev. **138**, A924 (1965).

⁸ V. S. Vavilov, A. F. Plotnikov, and G. V. Zakhvathin, Fiz. Tverd. Tela **1**, 894 (1959) [English transl.: Soviet Phys.—Solid State **1**, 894 (1959)].

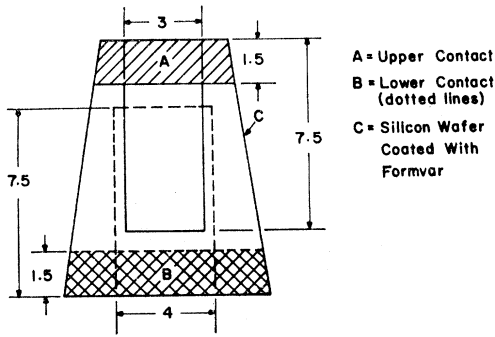


FIG. 1. Sample preparation.

kc/sec square wave, in bursts of duration of 600 μ sec, with a repetition rate of 400/sec. At this high frequency (200 kc/sec) the insulating films played the roll of a very large capacitor, but at the same time they prevent carrier injection into the semiconductor. Moreover, the high frequency also tends to short circuit surface barriers, thus leading to a uniform field distribution in the sample.

The electronic detection system was designed with the following requirements in mind: (1) High sensitivity is needed. (2) For small values of $\Delta\alpha$, the change in the absorption coefficient $\Delta\alpha$ is related to the variations ΔI_T in the intensity of the light going through the sample by the relation

$$(\Delta\alpha)d = (\Delta I_T / I_T)(1 + M), \quad (1)$$

where d is the length of the light path, and M is a value representing the effect of the internal reflections of the light in the sample. Thus the system was designed to measure $\Delta I_T / I_T$. (3) The temperature variations of the sample caused by the heating result in changes in the absorption coefficient in addition to the change caused directly by the electric field. The system was designed to distinguish between the two effects.

The electronic system is schematically described in Fig. 2. The light of a monochromator after passing through the sample is detected by the PbS detector. The ac component of the light intensity (with basic frequency 400 sec^{-1}), which is caused by the electric field

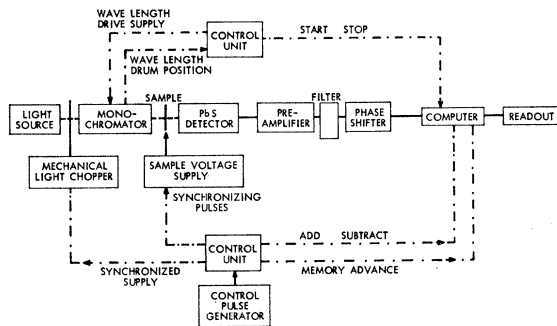


FIG. 2. Schematic description of the electronic detection system.

bursts applied to the sample, is amplified and after proper phase-shifting it enters the special-purpose computer.

The computer performs both the synchronous detection and the long-time integration in the following manner: The signal entering the computer is converted into a train of pulses the frequency of which varies, around a certain value, proportionately to the instantaneous voltage of the incoming signal. The pulses then can be either subtracted or added as beats to the memory. Pulses which convert the mode of operation of the computer from "add" to "subtract," and vice versa, are supplied by the same control pulse generator which controls the burst envelope of the field applied to the sample. Thus for one-half of the basic period of the electric field applied to the sample the computer is in the "add" mode, whereas for the second half it is in the "subtract" mode. It is easily seen that the number of beats in a memory address is given by

$$n(N) = \sum_{m=0}^{N-1} \left[\int_{mT}^{mT+T/2} (r_0 + \rho V_i(t)) dt - \int_{mT+T/2}^{(m+1)T} (r_0 + \rho V_i(t)) dt \right], \quad (2)$$

where NT is the total time spent in the address, r_0 is the center frequency of the pulse train, and $\rho V_i(t)$ is the deviation frequency. It is evident from Eq. (2) that $n(N)$ is proportional to the synchronous detection and integration over a period NT of the signal V_i . This is known to improve signal to noise ratio as \sqrt{N} . The computer is triggered to switch from one address to another at equal intervals of time while the wavelength drum in the monochromator is advanced uniformly. As a result we obtain values $\Delta J(\gamma)$ proportional to ΔI_T , as a function of wavelength drum setting.

Long integration times are usually difficult to achieve,

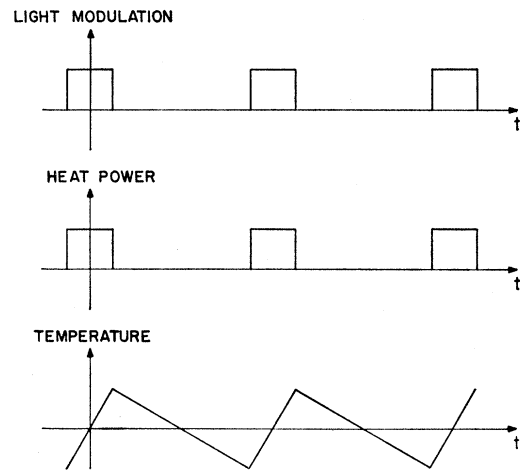


FIG. 3. The light intensity, heat supply to the sample, and temperature of the sample as functions of time.

owing to unavoidable drifts. As shown in the Appendix, the effect of the drift can be reduced greatly. This is achieved by measuring $\Delta J(\gamma)$ over the range of interest of γ with relatively short integration times for each measurement, but repeating the measurements many times. Moreover, these measurements are performed with γ alternately increasing and then decreasing as a function of time, by using oppositely directed wavelength drum drives. The results of all these measurements are automatically averaged by the computer, resulting in a measurement $\Delta J(\gamma)$ with an effective long integration time *and* small drift. Effective integration times of up to one hour per address, without any significant drift problems, have been achieved.

By chopping I_T in a square-wave form, synchronized with the control pulse generator, and detecting it with the same system, values of $J(\gamma)$ are obtained which allow us to relate $\Delta J(\gamma)/J(\gamma)$ to $\Delta I_T/I_T$ as follows.

$$\Delta I_T/I_T = \Delta J(\gamma)/J(\gamma) \sin(\pi D), \quad (3)$$

where D is the ratio between the duration of the applied field and the basic cycle time. Auxiliary measurements were performed to evaluate M , which turns out to be $\sim 10\%$.

The intensity modulation of the light caused directly by the electric field, the heat supplied to the sample, and the temperature variation of the sample as functions of time are shown in Fig. 3. The temperature drop while

the field is off is very close to a straight line since the cooling time is very short compared to the cooling time-constant of the sample. It is easily observed then that the first harmonic of the temperature is 90° out of phase with respect to the first harmonic of the light modulation caused directly by the electric field; and the first harmonic of the light modulation caused by the temperature variations bears a similar phase relationship to the desired modulation. Since the detection system is phase sensitive, the 90° phase difference was used to distinguish between the two effects. In order to adjust the phase of the whole detection system properly in agreement with that of the electric field bursts, we use a GaAs diode as a light source, turned on at exactly the same time that the electric field is applied. In this way the temperature effect intruding into the measurement of the field effect is reduced by a factor of 40 with respect to its original value.

RESULTS

Measurements of $\Delta\alpha$ as a function of photon energy caused by electric field intensities of 1.6×10^4 V/cm, 2.5×10^4 V/cm, and 3.8×10^4 V/cm are shown in Figs. 4, 5, and 6, respectively. Since the measurement was recorded as a sequence of noise-independent point values, the scatter of the points indicates correctly the amount of noise present in the results. The density of the points was chosen to be slightly larger than the resolution yielded by the monochromator.

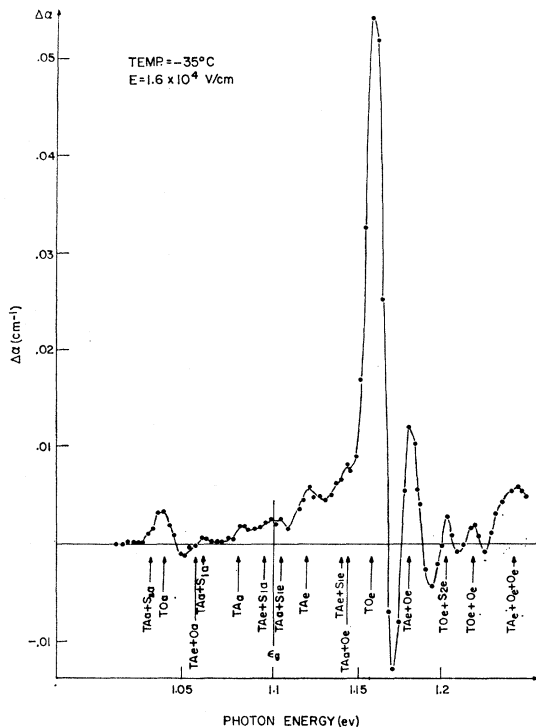


FIG. 4. Change of absorption as function of energy for applied electric field of 1.6×10^4 V/cm at -35°C . Notation of phonons as used by Chynoweth (see Ref. 5). Subscript e indicates emission of a phonon and subscript a indicates absorption of a phonon.

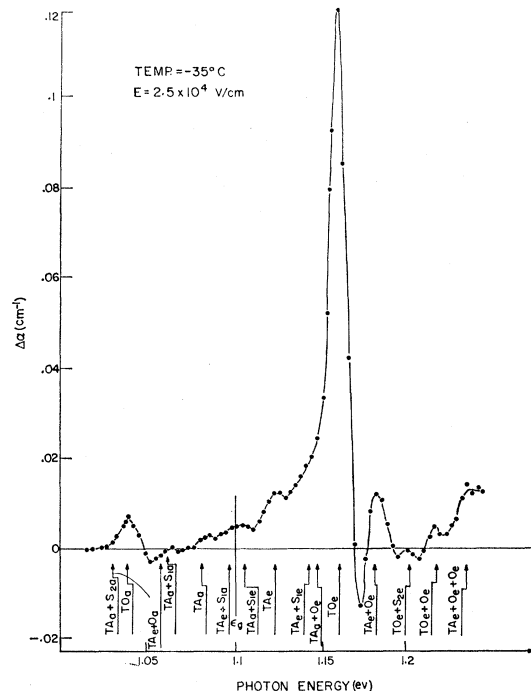


FIG. 5. Change of absorption as function of energy for applied electric field of 2.5×10^4 V/cm at -35°C . Notation of phonons as used by Chynoweth (see Ref. 5). Subscript e indicates emission of a phonon and subscript a indicates absorption of a phonon.

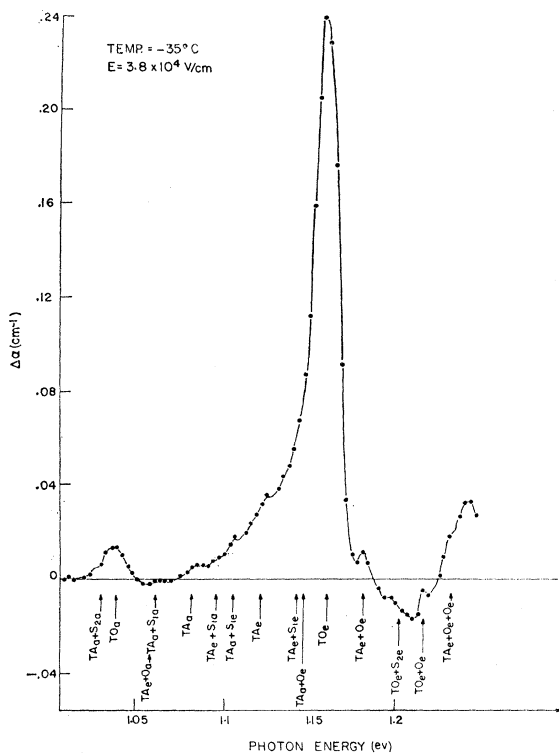


Fig. 6. Change of absorption as function of energy for applied electric field of 3.8×10^4 V/cm at -35°C . Notation of phonons as used by Chynoweth (see Ref. 5). Subscript e indicates emission of a phonon and subscript a indicates absorption of a phonon.

Comparing Figs. 4, 5, and 6, the following is quite clear: (1) The peaks indicated by arrows in Fig. 4 appear essentially at the same photon energy values in Figs. 5 and 6. (2) The peaks broaden considerably when going from lower to higher electric fields.

The theory of indirect transitions with applied electric fields⁶ predicts that for each phonon process, $\Delta\alpha$ versus photon energy should display a series of decaying peaks and also that $\Delta\alpha$ for a given process satisfies the relation:

$$\Delta\alpha = E^{4/3} F[(\epsilon_l + \epsilon_s - \epsilon_{\rho 0})/E^{2/3}], \quad (4)$$

where E is the electric field, ϵ_l is the photon energy, ϵ_s is the phonon energy (positive for absorption, negative for emission), and $\epsilon_{\rho 0}$ is the minimum energy gap. It follows from Eq. (4) that the photon energy corresponding to the summit of the peak is given by

$$(\epsilon_l + \epsilon_s - \epsilon_{\rho 0})/E^{2/3} = K_i, \quad (5)$$

where $F'(k_i) = 0$ and K_i is independent of E . Thus the difference in photon energy between summits of different peaks corresponding to the same phonon process should increase as $E^{2/3}$, whereas the position in energy of the first peak of each different phonon process should remain almost unaltered, because $(\epsilon_{l1} + \epsilon_s - \epsilon_{\rho 0})$ for this peak is very small. Thus if any two peaks shown in Fig. 4 belonged to the same process, their distance in

energy in Fig. 6 should have been 1.8 times larger than in Fig. 4. This is clearly not the case. The peaks are therefore interpreted in agreement with Frova and Handler⁴ as involving the absorption and emission of different phonons.

The width of the main peak as measured for example at the half power points is given by $\Delta\epsilon_1$

$$\Delta\epsilon_1 = E^{2/3} W, \quad (6)$$

where $W = |W_1 - W_2|$; $F(W_1)/F(k_1) = \frac{1}{2}\sqrt{2}$; $F(W_2)/F(k_1) = \frac{1}{2}\sqrt{2}$. Thus the width is proportional to $E^{2/3}$ which explains the observed broadening. The broadening of the peaks at higher fields is also the reason for not resolving the peak designated $TA_e + S_{1e}$ in Figs. 5 and 6.

It should be stressed that while the secondary positive peaks are not observed, the first negative peaks which should appear right after the first positive peaks are for certain processes clearly observed in Fig. 4. These peaks tend to disappear as a result of the broadening and overlap of the positive peaks at higher fields.

The interpretation of the different peaks is shown in Fig. 4 and the values of the phonon energies found in this experiment are compared with those found by Frova and Handler,⁴ Chynoweth *et al.*,⁵ and those calculated from Brockhouse's⁹ data, in Table I. It should be noticed that the accurate prediction of the location of the peaks on the grounds of Brockhouse's⁹ data is not straightforward for the multiphonon transitions. This is because the only conservations required are total energy and total momentum. Thus to obtain the accurate location of the peak, a calculation which takes into account both the shape of the electro-optic effect for a given phonon, and the density of states of all possible momentum combinations of the branches involved, should be carried out.

A few points should be stressed: We do not observe the peak corresponding to the absorption of $TA + TO'$. The large size of this peak in Handler's data appears odd because it should have required the co-existence of a peak corresponding to the emission of $TA + TO'$ with a magnitude of at least 0.03 cm^{-1} , which clearly does not exist. In the high-energy side we were able to resolve the peaks corresponding to $TO_e + S_{2e}$, $TO_e + O_e$, and $TO_e + O_e + O_e$. (The notation is the same as used by Chynoweth *et al.*⁵). In the vicinity of the energy gap we observe, in addition to the absorption and emission of the TA phonon, also two peaks at $\pm 40.6 \text{ meV}$ and one at 0 meV . The peaks at $\pm 40.6 \text{ meV}$ correspond in energy to the absorption and emission of $TA + S_1$. However, they also correspond to the absorption of TA and emission of O and to the emission of TA and the absorption of O which should exist because of the existence of a strong peak corresponding to the emission of $TA + O$. The peak at 0 meV might be the result of phonon-free processes or of the processes $TA_e + S_{1a}$ and $TA_a + S_{1e}$, both of which have almost zero energy. To

⁹ B. N. Brockhouse, Phys. Rev. Letters 2, 256 (1959).

TABLE I. Phonon energies in Si in meV.

		TA	TA+S ₁	TO	TA+S ₂	TA+O	TO+S ₂	TO+O	YO+O+O
Keldysh effect (Ref. 4)	Room temp.	17.5		58.1	66	84			
	92°K			57.5		84.1	102.3		
Tunnelling (Ref. 5)	4°K	18.4		57.6	65.4	83.1	102	121	141
Neutron scattering (Ref. 8)		18.2	41.2	57.8	64.4	81.5	103.6	120.7	144.6
Present work	-35°K	18.8	40.6	57.4	64.9	79.7	102.8	119.9	142

resolve these possibilities a measurement at -191°C was performed with the result presented in Fig. 7. It is seen that all the peaks below the one at 18.8 meV vanish whereas all the rest including the one at 40.6 meV remain. It can therefore be concluded that all the peaks below $+18.8$ meV are caused by processes which involve the absorption of a phonon, whereas the peaks at and above $+18.8$ meV should be caused by phonon emission processes only. Thus the peak at 40.6 meV is interpreted as composed of $\text{TA}_e + \text{S}_{1e}$ and $\text{TA}_a + \text{O}_e$ and the peak at zero as the double peak $\text{TA}_e + \text{S}_{1a}$ and $\text{TA}_a + \text{S}_{1e}$.

The results for the magnitude of the peak corresponding to TO_e are shown in Fig. 8 on a log-log scale. The curve appears to be close to a straight line with an average slope of 1.72 but there are significant departures from this slope. From Eqs. (4) and (5) we see that $\Delta\alpha$ measured at its summit is proportional to $E^{4/3}$. Thus our experimental results show a larger slope than theoretically predicted though it is smaller than the slope of 2 previously reported.^{3,4}

Current work suggests that the deviation from the theoretical dependence on the electric field and the absence of the secondary peaks might possibly be

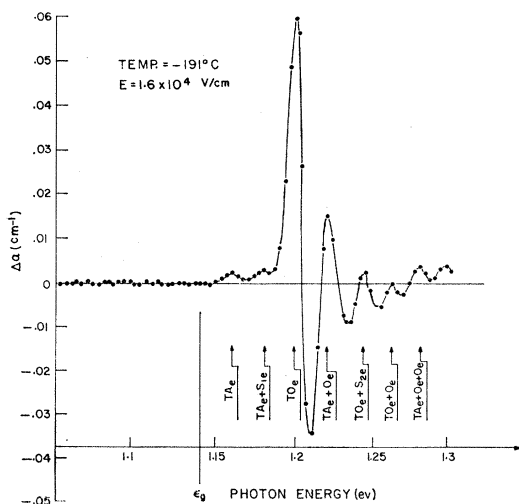


FIG. 7. Change of absorption as function of energy for applied electric field of 1.6×10^4 V/cm at -191°C . Notation of phonons as used by Chynoweth (see Ref. 5). Subscript e indicates emission of a phonon and subscript a indicates absorption of a phonon.

explained by the existence of strong electric fields in the crystal of the type discussed by Redfield.¹⁰

SUMMARY AND CONCLUSIONS

A method for making bulk measurements of the Keldysh effect has been developed. This method can be used for materials of considerable resistivity ($5 \times 10^4 \Omega \text{ cm}$ and higher) and it is usable in cases where junction techniques are not available. In fact, this method is now being used on other materials such as TiO_2 for which preliminary results have already been obtained.

An improvement in the sensitivity of the detection system compared to that of previously reported systems

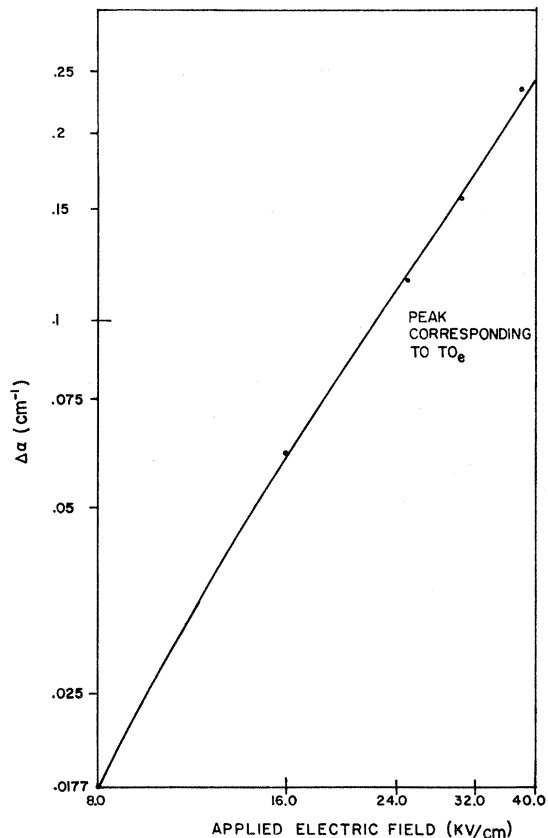


FIG. 8. Change of absorption for the peak corresponding to TO_e process as function of applied electric field.

¹⁰ D. Redfield, Phys. Rev. **130**, 914 (1963).

has been obtained by very long integration times with negligible drift. This was achieved by the proper averaging of many measurements of $\Delta\alpha$ versus photon energy by a special purpose computer.

As a result of the higher sensitivity and consequently the possibility of working with higher resolution several processes not previously observed before were resolved, specifically TO_e+O_e ; $TA_e+O_e+O_e$; TA_e+S_{1e} ; TA_a+S_{1a} ; TA_a+S_{1e} ; and TA_e+S_{1a} . It is plausible that with a further improvement in the measurement additional processes may be resolved.

The size of the main peak has been found to be closely proportional to $E^{1.72}$. The fact that this result deviates from previously published results^{3,4} ($\Delta\alpha \propto E^2$) shows that the deviation from the theory might not be fundamental. One possible explanation for the deviation from theory is the existence of internal electric fields originating from impurities and imperfection.¹⁰ This possibility is being presently explored.

ACKNOWLEDGMENTS

I would like to thank Professor R. B. Adler from the Massachusetts Institute of Technology for the supervision of this work and his great help in its different phases. I also want to thank W. Brennan for his great help in building the electronic equipment and Dr. S. H. Fang for his help in the performance of the low-temperature measurement.

APPENDIX

Let the position of the wavelength drum be denoted by γ with the range of interest being between $\gamma=0$ and $\gamma=1$. Let the basic period of the field applied to the sample be T ($T=1/400$ sec). The computer spends $\frac{1}{2}T$ in the "add" mode and $\frac{1}{2}T$ in the "subtract" mode. Let the net number of beats added to the memory in time T , originating from the true signal, be $R(\gamma)$. We denote the over-all term of measurement by τ . During this time γ varies P times from 0 to 1 and back from 1 to 0. If the number of addresses used is M , then the total number of beats in the address number γM is

$$n_s = R_s(\gamma)\tau/MT, \quad (\text{A1})$$

which is independent of P .

In addition to the true signal and the noise there is also a drift signal. Drift might enter for example from varying parasitic coupling between the generator which supplies the voltage to the sample and the system, or, in the processes of synchronous detection and in other ways.

We can represent the drift in our system as adding $R_d(t)$ to the memory in the period T . It should be noticed that R_d is independent of γ and of P . The number of beats added to the address number γM because of the drift signal is given by

$$n_d(\gamma) = \sum_{m=1}^P [R_d(m\tau/P + \gamma\tau/2P) + R_d(m\tau/P + (2-\gamma)\tau/2P)]\tau/2PMT. \quad (\text{A2})$$

Let us expand $R_d(m\tau/P + \Delta t)$ in the form

$$R_d(m\tau/P + \Delta t) = R_d^{(0)}(m\tau/P) + R_d^{(1)}(m\tau/P)\Delta t + R_d^{(2)}(m\tau/P)\Delta t^2. \quad (\text{A3})$$

Substituting Eq. (A3) into Eq. (A2) we obtain

$$n_d(\gamma) = \sum_{m=1}^P [R_d^{(0)} + R_d^{(1)}\gamma\tau/2P + R_d^{(2)}(\gamma\tau/2P)^2 + \dots + R_d^{(0)} + R_d^{(1)}(2-\gamma)\tau/2P + R_d^{(2)}(2-\gamma)^2\tau^2/4P^2 + \dots]\tau/2PMT. \quad (\text{A4})$$

For relatively large values of P

$$\sum_{m=1}^P R_d^{(2)}(m\tau/P)\tau/2PMT \approx (1/4MT) \left[\frac{dR_d}{dt} \Big|_{t=\tau} - \frac{dR_d}{dt} \Big|_{t=0} \right]. \quad (\text{A5})$$

The right-hand side of Eq. (A5) is independent of P . We can therefore conclude from Eq. (A4) that terms of the drift $n_d(\gamma)$ which depend on γ decrease at least as $1/P^2$. This shows that dividing the total measurement time τ into a large number of wavelength drum cycles P , effectively reduces the drift which is not uniform in photon energy. It is very easy to determine the value of the drift which is independent of photon energy, for example, by a zero measurement at the beginning of each cycle, achieved by turning the light off.